Preferred citation: P. Huber, S. Nivelon, P. Ottenio, M. Schelcher and A. Burnet. Prediction of mineral deposits in kraft pulp bleaching lines through chemical process simulation. In **Advances in Pulp and Paper Research, Oxford 2017**, *Trans. of the XVIth Fund. Res. Symp. Oxford, 2017*, (W. Batchelor and D. Söderberg, eds), pp 451–485, FRC, Manchester, 2018. DOI: 10.15376/frc.2017.1.451.

PREDICTION OF MINERAL DEPOSITS IN KRAFT PULP BLEACHING LINES THROUGH CHEMICAL PROCESS SIMULATION

Patrick Huber, Sylvie Nivelon, Pascal Ottenio, Matthieu Schelcher and Auphélia Burnet*

CTP, CS90251, 38044 Grenoble Cedex 9, France

ABSTRACT

The general tendency in the pulp industry towards reduced fresh water consumption and minimum effluent causes major deposit problems in mills. Chemical pulp bleach plants are affected by several types of mineral deposits, the most frequent being calcite, calcium oxalate and barite. We present a coupled chemical process simulation of a kraft pulp bleaching line, which handles chemical equilibria, together with dissolution and precipitation effects. The simulation could adequately predict formation of mineral deposits throughout a D0(EP)D1D2 bleaching line. Strategies to help reduce formation of calcium oxalate and barite scales could be evaluated. Partial substitution of sodium hydroxide by a magnesium source at extraction stage is anticipated to inhibit formation of calcium oxalate throughout the line. Also, using sulfuric acid instead of spent acid for pH regulation at D0 would reduce but not suppress barite deposits.

* Corresponding author: Patrick.Huber@webctp.com

1 INTRODUCTION

The pulp industry has made great efforts to reduce its specific water consumption over the last few decades. With the increasing closure of bleach plants in chemical pulp mills, many dissolved species accumulate in process loops, which may lead to scale deposits. These may plug washing devices and severely impact the productivity of the fibre line. Various methods may be used to prevent deposits, such as metal removal (by acid washing and/or chelation). In severe cases, the bleach plant has to be shut down, as only hydro-blasting techniques and/or acid cleaning procedures can remove the most encrusted deposits.

The most frequent types of scale in bleaching lines are calcite (calcium carbonate), hydrated calcium oxalate and barite (barium sulphate) [1].

Calcite: $$CaCO_{3(s)} \leftrightarrow Ca^{+2} + CO_3^{-2} \quad (1)$$

Calcite deposits form in supersaturated solutions containing both calcium and inorganic carbon. The main source of calcium is the wood material itself (0.5–1.0 kg/a.d.T [1]). Calcium is released during the cooking stage. Carbonate ions mostly come from the white liquor (as carry-over from the re-caustification cycle). In bleach plant filtrates, various dissolved organic species can complex with calcium, thus reducing free calcium available for precipitation.

Calcium oxalate: $$CaC_2O_4{:}\ H_2O_{(s)} \leftrightarrow Ca^{+2} + C_2O_4^{-2} + H_2O \quad (2)$$

Calcium oxalate deposits form in supersaturated solutions containing both calcium and oxalate. Oxalic acid ($C_2O_4H_2$) is a dicarboxylic acid naturally present in wood (0.2–0.8 kg/a.d.T, and up to 20–30 kg/a.d.T in bark) [2]. It is also formed from reactions with wood during bleaching as an oxidation product of lignin (mainly) and hemicelluloses (xylan/uronic acids) (to a lesser extent). Oxalic acid formation is proportional to Kappa number reduction [3]. Typically, the largest oxalic acid release occurs during oxygen delignification and ozone bleaching stages. Like other dissolved wood organics, oxalate plays the role of a weak chelating agent with respect to most metal cations.

Barite: $$BaSO_{4(s)} \leftrightarrow Ba^{+2} + SO_4^{-2} \quad (3)$$

Barite deposits form in supersaturated solutions containing both barium and sulphate ions. The main source of barium in the bleaching line is the wood itself. There are large differences among wood species, but typically there is more barium in hardwood chips (20–60 ppm) than in softwood chips (10 ppm) [4]. As in the case of the other metal cations, the barium content of the bark is much

higher than that of the stem wood. The main source of sulphate in the bleaching line is pH regulation with sulphuric acid.

In order to reduce scaling, it is crucial to understand the physicochemical parameters that govern the phenomenon, in the conditions of a closed bleach plant (i.e. at high ionic strength, and in the presence of dissolved wood organics and fibres). Chemical speciation methods are an invaluable way of predicting scaling risks [5], [6]. Various dedicated chemical programs may be used for this purpose: CHEMSHEET [7], FRENCHCREEK [5], OLI [8], [9], ORCHESTRA [10], PHREEQC [11], SOLGASWATER [12], Visual MINTEQ [13] and others.

Classical process simulations resolve mass and heat balances, but do not account for chemical equilibria. On the other hand, chemical speciation methods can help to determine local scaling risks in a given process, but do not help to predict the consequences of a process modification as such. To resolve this issue, bridges between process simulation software and chemical speciation engines have been developed in order to take into account electrolyte chemistry problems.

Coupled chemical simulations have been developed for papermaking processes. These include BALAS-CHEMSHEET [14], [15], WinGEMS-SOLGAS-WATER [16], [17] and PS2000-PHREEQC [18]. This extends the capabilities of the process simulation, and makes it possible to accurately take into account dissolution and precipitation phenomena.

There has been on-going interest for alternative alkali sources in bleaching lines, sometimes with a view to reduce mineral deposits. Magnesium hydroxide has long been proposed for the bleaching of mechanical pulps: main advantages compared to caustic soda include reduced COD load [19], and reduced calcium oxalate scale [20], [21]. For chemical pulp bleaching, partial replacement of sodium hydroxide by magnesium hydroxide or magnesium oxide in extraction stages is possible for softwood: the end pH is typically lower (–1 pt), at similar brightness [22], [23], [24]. In this case, the released COD may be considerably reduced [25]. Depending on caustic soda price variation, the substitution by magnesium oxide may become economical [23]. Addition of magnesium salts in general has been also been proposed as a way of reducing deposits of calcium oxalate. The use of $MgSO_4$ in D bleaching stages of chemical pulp was simulated [26]. It was shown that adding a small amount of $MgSO_4$ (1 kg/t) at the inlet of the D0 stage could maintain the concentration of free oxalate in the system. This was expected to limit deposits of calcium oxalate, although no mill trials could be performed.

The objective of this study is to develop a simulation of mineral precipitates in a bleaching line. This makes it possible to evaluate strategies to limit the formation of mineral deposits. The study was carried out at the Fibre Excellence Saint Gaudens pulp mill.

2 MATERIALS AND METHODS

2.1 Analytical methods

The pH, temperature, and conductivity were measurement in-situ (WTW multi 340i). Pulp samples were hot squeezed on-site to produce a wet pulp pad and filtrates. The filtrates were immediately filtered to produce aliquots for analytical measurements. The rapid sampling procedure prevented the cooling of the samples, and limited the precipitation of calcium oxalate (which would have been lost in the filtrates analysis).

Several vials were prepared on site for further analyses:

- Metal cations: filtered over syringe filter (0.45 μm, HPF Millex, Millipore), adjusted to pH = 2, with nitric acid (65%), according to NF EN ISO 5667–3, 2013;
- Oxalate: filtered over syringe filter (0.45 μm, HPF Millex, Millipore), adjusted to pH = 2, with hydrochloric acid (37%), according to SCAN-N39:05;
- Inorganic carbon, and anions (chloride, sulphate): filtered over syringe filter (0.45 μm, Millex LCR, Milipore), vial filled to the brim to prevent degassing (pH adjustment.

The wet pulp pads obtained from the hot squeezing procedure were dried, and incinerated (425 °C, 4 h). The ashes were dissolved in hydrochloric acid, and analysed for total cations content. The amounts of cations in solid form (including both precipitates and bound to fibres) were calculated by difference between total amounts in pulp pads and in the liquid fraction.

Metal cations were analysed by Inductively Coupled Plasma-Atomic Emission Spectroscopy (ICP-AES) (5100 Agilent technologies), according to NF EN ISO 11885, 2007.

Inorganic carbon was analysed by Infra-Red absorption in gas-phase after acidic outgassing (TOC-V csn, Shimadzu), based on NF EN 1484, 1997.

Anions and oxalate were analysed by ionic chromatography (Dionex DX500 composed of an electrochemical detector ED50, gradient pump GP50, thermal compartment AS50 and an autosampler AS50), according to NF EN ISO 10304–1:2009 and SCAN-N39:05.

Suspended solids in pulps were measured after filtration (ash-free paper filter, PROTEIGENE DP5891090) and oven heating (105°C).

COD was measured with WTV micro-kits.

Fibre charge was determined using conductometric titration, following a method adapted from ref. [27] (washing with deionized water, acid washing step in hydrochloric acid 0.1 M at 0.6% consistency for 1 h to desorb metal cations and fully protonate the fibres, washing with deionized water, dilution to 0.3%, adjustment to

pH = 2 with hydrochloric acid, titration with caustic soda 0.1 M, and recording of conductivity).

Deposits were characterised by X-ray microanalysis for elemental composition (energy-dispersive spectrometer (EDS) mounted on a scanning electron microscope JEOL JSM 6400), and by X-ray diffraction for crystallographic analysis (XRD, PANalytical X'Pert Pro MPD system, Cu Ka radiation, $\lambda = 1.54056$ Å, phase identification with International Centre for Diffraction Data (ICDD) database).

2.2 Chemical speciation methods

Scaling is a complex phenomenon, involving many dissolved species, together with solid and gas phases. The scaling potential of a solution is defined by its supersaturation [28]. Supersaturation quantifies how far the solution is from equilibrium.

In an aqueous solution, a chemical element may be involved in several chemical reactions, so that it is distributed as various soluble species. Thus, only a fraction of the element participates in the scaling process. For instance, in the case of calcium carbonate scaling, only a fraction of the total inorganic carbon is actually in carbonate form, and this depends on carbonic acid equilibria, thus mainly on pH.

In order to estimate scaling, the saturation index with respect to the precipitating phase has to be calculated. This involves estimating the ionic activity product (IAP), i.e. the activities of the precipitating species in the solution (for instance with calcite: $IAP = a(Ca^{+2}).a(CO_3^{-2})$, where a() denotes activity). This is achieved through the simultaneous resolution of all chemical equilibria in the system. The ionic activity product can then be compared with the solubility product Ks, and the ratio is the supersaturation ($S = IAP/Ks$). The saturation index (SI) is defined as log(S). If a solution has $SI < 0$, there is no scaling risk, as it could dissolve more solids before reaching equilibrium. If a solution has $SI > 0$, there is a scaling risk, as it would tend to precipitate some solid in order to reach equilibrium (which corresponds to $SI = 0$).

In this work, all speciation calculations were performed with PHREEQC [11]. The simulation handles a 3-phase system (solid–liquid–gas phases) (Figure 1).

The four considered mineral phases (Calcium carbonate, calcium oxalate, barium sulphate and magnesium hydroxide) can dissolve in or precipitate from the liquid phase. Calcium oxalate, barium sulphate and magnesium hydroxide are considered to be in equilibrium with the system (i.e. supersaturation is not allowed). On the other hand, calcium carbonate requires a high supersaturation to precipitate, so that only dissolution is allowed by default. Therefore, the system can be supersaturated with respect to calcium carbonate, unless a local precipitation is allowed.

The fibres have a surface charge (arising mostly from –COOH from hemicelluloses) that exchanges metal cations with the solution. The total ion exchange

capacity depends on the pH, as the –COOH groups are ionised in alkaline media, and protonated in acidic conditions. The ion exchange reactions are defined with respect to calcium as in ref. [29], using the EXCHANGE feature in PHREEQC (where Y represents the exchange site):

- $Ba^{+2} + CaY_2 = BaY_2 + Ca^{+2}$, log K = –2.4
- $Mg^{+2} + CaY_2 = MgY_2 + Ca^{+2}$, log K = –0.8
- $Na^{+} + 0.5\ CaY_2 = NaY + 0.5\ Ca^{+2}$, log K = –0.7
- $H^{+} + 0.5\ CaY_2 = HY + 0.5\ Ca^{+2}$, log K = 2.0

Thus the affinity of cations for fibres can be ranked as follows: $H^{+} > Ca^{+2} > Na^{+} > Mg^{+2} > Ba^{+2}$.

Bleaching reactions release dissolved wood organics which play a role in the chemical speciation of the whole system. For instance, oxalate formed from the oxidation of lignin can precipitate with calcium, which forms deposits. Oxalate also complexes with other metal cations such as magnesium. Besides, bleaching reactions release various short chain organic acids. These are lumped into a general species which has particular dissociation constant (pKa = 3.5) and complexation constant with calcium (log K = 3.5) (values taken from ref. [30]). This is representative of the fact that calcium oxalate has a much higher apparent solubility in bleaching effluents than in pure water. In other words, the presence of dissolved wood organics limits the amount of formed deposits. Note that the effect of ionic strength on apparent solubility of mineral phases is taken into account by default in the simulation. In the same way, dissolved wood organics increase the apparent solubility of barium sulphate in bleaching effluent. Therefore, we have defined a complexation constant with barium (log K = 2.8), in accordance with literature data [31].

The concentration of the lumped "wood organics" was set equal to COD (g/L). It is difficult to set the molar mass of "wood organics". Using a molar mass of 60 g/mol (representative of a short chain organic acid such as acetic acid), we could recalculate a calcium complexation behaviour by "wood organics" similar to that reported in [30] (not shown).

Various chemicals can be injected to the system to simulate several bleaching operations, such as caustic soda, sulphuric acid, sodium sulphate, etc. (using the REACTION feature in PHREEQC). These chemicals have an effect on the pH and participate to all speciation reactions.

In several locations of the process, the system is in contact with air (i.e. atmospheric diffusers). Partial degassing is simulated by equilibrating inorganic carbon to an intermediate level of atmospheric CO_2 partial pressure.

The pH is imposed on all sources to the simulation. Then the local equilibrium pH results from the resolution of all above chemical equilibria.

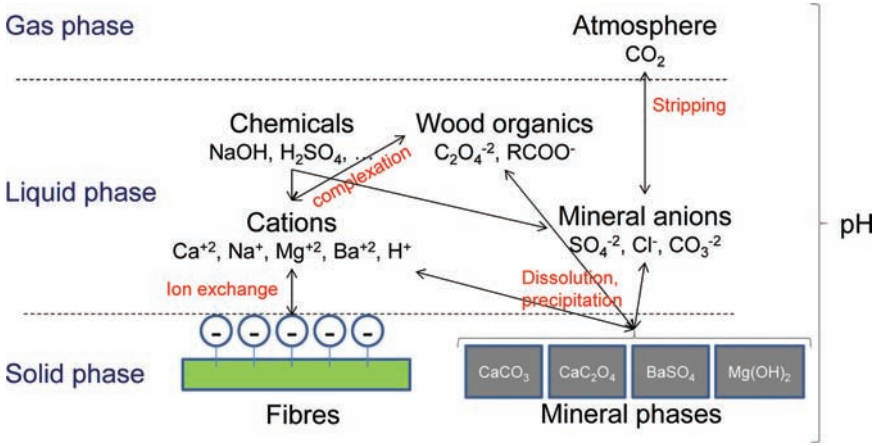

Figure 1. Schematic of the phenomena simulated with the chemical speciation methods.

It is well known that fibre charge decreases as a consequence of bleaching reactions. Therefore, we have developed a "charge reduction" module. The exchange species is initially introduced to the system with the brownstock. Then it is set to follow the fibres. In the charge reduction module, the total amount of exchange species is reduced (using the REACTION feature in PHREEQC with a negative coefficient), then the new equilibrium is recalculated. Typically, this leads to a decreased amount of cations on the fibres and releases more cations to the liquid phase.

2.3 Simulation methods

2.3.1 General principles

Our research group has been developing the PS2000 process simulation dedicated to papermaking processes under the G2 environment (Gensym). Briefly, a flow sheet of the mill was constructed with dedicated unit operations specific of the process. The full mill model was equilibrated by resolving flow and mass balances around each node and unit operation, for each simulated species. The mass balances were resolved iteratively, until the difference between two successive values of a species was lower than a pre-set tolerance. Separation coefficients were defined for some species on particular unit operations and adjusted to match measured concentration profiles. Also, some release coefficients were defined to simulate production of wood organics (including oxalic acid) as by-products of bleaching reactions. The fresh water was also considered as a source of dissolved species. Their concentration was adjusted against measured water quality. The

temperature was calculated from a classical enthalpy balance. Methods were further described in [32], [33].

2.3.2 Coupled chemical process simulation

In a chemical process simulation, the process simulation software and the chemistry engine are interfaced in a master/slave scheme. The process simulation software takes care of all heat and mass balances, for both suspended solids (fibres, fines, precipitates) and dissolved solids (COD, and all salts and dissolved organics). At each unit operation model, the chemistry engine is run with total chemical elements as input, and calculates the chemical speciation in the solution (including ion-exchange with fibres). The supersaturation levels calculated for the mineral phases can be used to determine the extent of precipitations or dissolutions. The resulting pH is propagated to the next flow as a non-balance parameter. The new total amounts of dissolved elements are passed back to the process simulation software for the next iteration. In the same way, the results of mixing two flows can be calculated (Figure 2).

2.3.3 Diffusion washer model

The mill uses atmospheric diffuser to wash the pulp at the end of the bleaching stage, so that an adequate model needed to be developed. The proposed model consists in 2 blocks (Figure 3). The first block performs a thickening operation: this simulates the displacement of the liquor from the pulp. The level of thickening

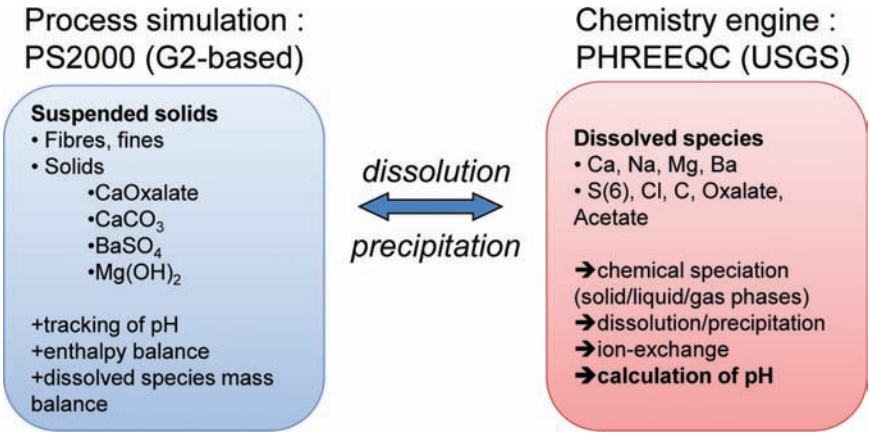

Figure 2. Principles of the coupling procedure between the process simulation software and the chemistry engine.

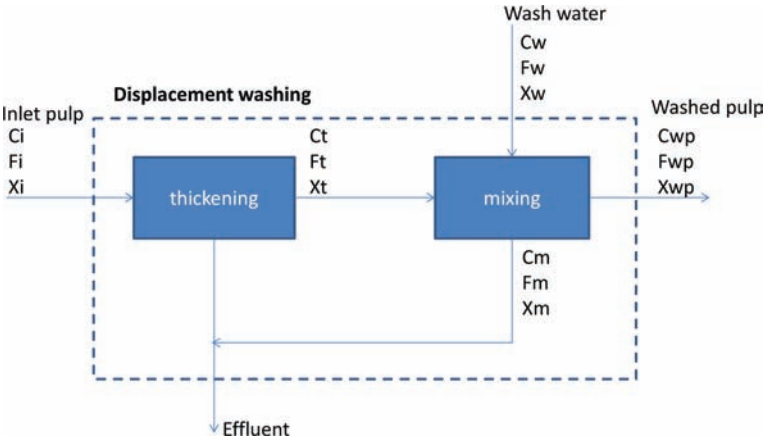

Figure 3. Model of displacement washing for the atmospheric diffuser (C: pulp concentration (g/L), F: water flows (m^3/h), X: concentration of dissolved species (g/L)).

is governed by the intermediate thickening consistency C_t. Then the thickened pulp is mixed with the wash water. At that point, we suppose that ideal mixing is achieved, and all chemical equilibria are resolved (precipitates can be formed or dissolved, metal cation can be exchanged with fibres, etc.). Formed precipitates are set to follow the washed pulp flow. The pulp is then thickened to the target consistency of the washed pulp C_{wp}. The 2 generated filtrates are mixed to form the bleaching effluent.

The possible consequences of aeration (i.e. CO_2 stripping in acidic conditions, or carbonatation in alkaline medium) are simulated afterwards, on effluent and washed pulp separately.

Note that the consequences of bleaching reactions themselves are simulated before the 2-block model, through the release of wood organics and oxalate.

The washing efficiency, or displacement ratio is mainly governed by the intermediate thickening consistency C_t, as detailed below.

By definition, the dilution factor for pulp is

$$DF = \frac{F_w - F_{wp}}{P} \tag{4}$$

and the displacement ratio for dissolved species is

$$DR = \frac{X_i - X_{wp}}{X_i - X_w} \tag{5}$$

The parameters of the diffusion washer model are: the intermediate thickening consistency C_t, and the washed pulp consistency C_{wp}. The wash flow F_W and the production P are fixed.

Writing the flow balance ($F_t + F_w = F_m + F_{wp}$) and the mass balance ($X_tF_t + X_wF_w = X_mF_m + X_{wp}F_{wp}$) around the mixing unit give:

$$DR = \frac{C_t C_{wp} DF + C_t}{C_t C_{wp} DF + C_t + C_{wp}} \tag{6}$$

and

$$DF = \frac{F_w}{P} - \frac{1}{C_{wp}} \tag{7}$$

This proposed model for the diffuser provided a satisfactory description of most dissolved species, with only one main adjustable parameter C_t, identical for all species. The outlet consistency is set according to field measurements. Note that the separation of dissolved species between pulp and filtrates is only governed by chemical and ion-exchange equilibria.

2.3.4 Model of the fibre line

The model represents the mill bleaching sequence D0(EP)D1D2, starting from the brownstock exiting the oxygen delignification stage (Figure 4). The pulp is washed in a counter current jump stage scheme, with separation of acidic and alkaline filtrates. The acidic chlorine dioxide stages are washed with the wire press water, while the alkaline EP stage is washed with hot raw water.

The mill uses up-flow bleaching towers with integrated atmospheric diffusers. This somewhat complicates the calibration of the model as it is not possible to sample the pulp just before the washing step itself. As mentioned earlier, the diffuser model consists of 2 blocks (thickening, followed by mixing with wash water). The intermediate thickening consistency has been adjusted to fit the measured COD profiles.

The injection of chemicals to the pulp is represented by the green droplet modules. The use of spent acid from the chlorine dioxide generator to acidify the pulp before the D0 and D1 stages, is simulated by the injection of pure Na_2SO_4 followed by pure H_2SO_4 (with a ratio 47:53, as measured on the spent acid). Injection of pure NaOH is simulated at EP and D2 stages inlet. Note that an additional source of CO_2 had to be implemented after the NaOH injection at EP inlet, in order to fit the measured inorganic carbon profiles. That is likely due to soda carbonatation during the preparation process (see later). In the same way, a source of CO_2

was implemented to the alkaline effluent. The flow of spent acid and caustic soda injection have been set according to the mill DCS values at the time of sampling.

Aeration modules had to be implemented on D0 and D1 stages outlets to simulate the stripping of inorganic carbon to the atmosphere that occurs in the atmospheric diffusers in acidic conditions. These are represented as blue droplets in the simulation. The equilibrium partial pressure of CO_2 was set to fit the measured inorganic carbon profiles. The CO_2 stripping in D2 stage was found to be negligible.

A precipitation module was implemented at EP inlet to force the precipitation of calcite in that supersaturated flow. The equilibrium SI was set to fit the measured calcium profiles. Recall that supersaturation is not allowed for either calcium oxalate, barite or magnesium hydroxide, so that minerals are formed by default down to equilibrium (SI = 0), anywhere in the circuits.

The release of wood organics that occurs during bleaching was simulated by implementing oxalic acid and wood organics injection at the inlet of each diffuser (represented by orange and brown droplet modules respectively). Recall that wood organics is an organic acid with high complexation power with respect to calcium and barium (as described in Section 2.2), that basically represents measured COD. The injected flow rates of oxalic acid were adjusted to fit the measured oxalate profiles. The injected flow rates of wood organics were set to fit the measured COD profiles.

The characteristics of the sources (brownstock, hot raw water, and white water from wire press) were set according to the field measurements (pH, temperature, elemental analyses, fibre charge, liquid/solid partition). The pH of the chlorine dioxide solution had to be adjusted to pH = 1.4 to fit the measured pH profile throughout the bleaching sequences (while the mill reported pH = 1.6).

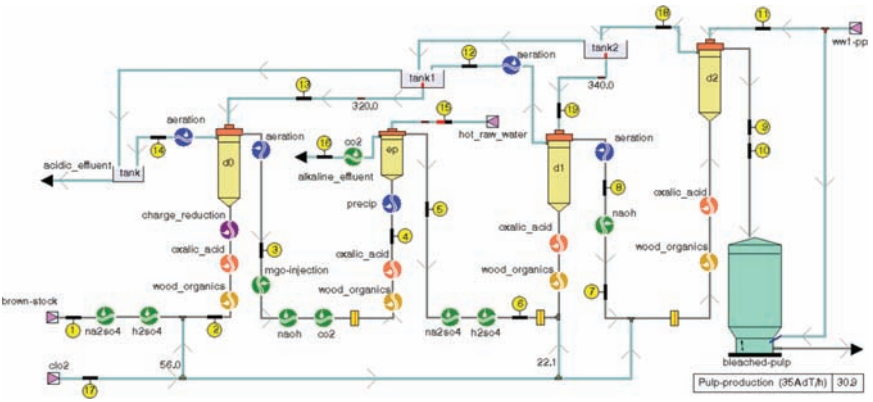

Figure 4. Screenshot of the developed process simulation (chemical injection modules and organics release are represented by coloured "droplet" logos; chemical equilibriums are resolved at each process node).

A fibre charge reduction module was implemented at D0 inlet, to reflect the measured reduction of fibres ion-exchange capacity.

3 RESULTS

3.1 Analytical results

Physico-chemical measurements on filtrates are reported in Table 1. Solid cations reported in Table 2 are calculated by difference between total cations in wet pulp and concentration in filtrates. The evolution of the measured profiles is discussed in Section 3.3.

From the chemical speciation, the saturation index with respect to the considered mineral phases has been calculated for each filtrate (Figure 5).

The process waters are clearly supersaturated with respect to calcite around the extraction stage. The SI(Calcite) is highest at "inlet EP". The reduced SI in "outlet EP" and "EP washing filtrate" is presumably caused by partial precipitation of Calcite (which immobilises Ca^{+2}, CO_3^{-2} and lowers the pH). The low SI in the wash waters suggests that the cause of the supersaturation lies just before the inlet of the diffuser, and right after caustic soda injection. These supersaturation calculations are corroborated by mill observations (calcite deposits found on the walls of the pipe to the inlet of EP diffuser, see Section 3.2).

The chemical speciation indicates that there is a risk of Calcium oxalate deposits in both EP and D2 stage inlet (= 'outlet D1'). Deposits of Calcium oxalate have indeed been found on the screen rings of the EP diffuser (see Section 3.2). However, the mill did not report deposit related problems in the D2 diffuser. It is possible that the hydraulic configuration of the D2 washer does not promote the adhesion of the formed calcium oxalate crystals (in other words, calcium oxalate is formed but flows away with the pulp, which shows SI(calcium oxalate) = 0 as a result of precipitation).

Barite is anticipated to precipitate in the D0 stage and the D2 stage. The mill indeed reported barite deposit problems on the D0 diffuser screen. No deposits were reported for the D2 stage. Again, it is possible that in the conditions of the D2 stage, the barite precipitates in the pulp flow and hopefully does not form deposits.

The total fibre charge measured from conductometric titration decreases from 85 meq/kg for the brownstock down to 60 meq/kg as a result of D0 bleaching (Figure 6). That is explained by the dissolution of charged groups from the fibres. Then the charge is essentially stable, with a slight decrease after D2 bleaching. The charge of the brownstock has been used as the reference value for the simulation. The variation of fibre charge has been considered in the calculations.

Table 1. Analytical measurements on filtrates

Filtrates	pH	°C *Temp*	µS/cm *Cond.*	g/L Ca	g/L K	g/L Mg	g/L Na	mg/L Ba	g/L C	g/L Cl	g/L *Sulfate*	g/L *Oxalate*	g/L COD
brownstock	10.33	40.9	2071	0.006	0.038	0.005	0.456	0.040	0.077	0.017	0.174	0.016	1.426
outlet D0	3.05	51.0	3790	0.149	0.031	0.048	0.589	0.117	0.004	0.493	0.764	0.049	0.873
inlet EP	10.74	53.6	7110	0.097	0.026	0.027	1.610	0.101	0.105	0.435	0.745	0.079	2.170
outlet EP	9.45	60.2	1859	0.031	0.008	0.012	0.384	0.256	0.037	0.097	0.154	0.018	0.611
outlet D1	4.29	54.0	2980	0.127	0.012	0.023	0.542	0.103	0.002	0.391	0.503	0.024	0.514
outlet D1 (+caustic)	4.66	58.0	3085	0.117	0.011	0.022	0.551	0.109	0.002	0.321	0.465	0.023	0.513
outlet D2	4.28	46.5	1716	0.071	0.006	0.009	0.289	0.115	0.001	0.148	0.346	0.011	0.188
D2 washing	4.03	42.8	1391	0.066	0.005	0.006	0.246	0.119	0.001	0.095	0.311	0.008	0.123
D2 washing filtrate	4.23	66.2	2825	0.112	0.012	0.019	0.536	0.132	0.010	0.378	0.407	0.013	0.429
D1 washing filtrate	4.95	67.5	2570	0.117	0.010	0.033	0.461	0.154	0.018	0.300	0.217	0.023	0.699
D0 washing	4.83	67.9	2590	0.116	0.010	0.032	0.453	0.136	0.015	0.317	0.220	0.020	0.636
D0 washing filtrate	2.42	56.9	5095	0.165	0.049	0.073	0.663	0.060	0.028	0.397	1.037	0.057	1.422
EP washing	7.67	67.2	177	0.031	0.001	0.002	0.000	0.335	0.014	0.005	0.008	0.001	0.000
EP washing filtrate	9.56	65.2	5000	0.045	0.022	0.008	1.175	0.120	0.087	0.367	0.534	0.060	1.732

Table 2. Analytical measurements on pulps

Pulps	g/L *Susp. solids*	mg/kg Ca	mg/kg K	mg/kg Mg	mg/kg Na	mg/kg Ba
brownstock	109.6	1916	215	805	1411	0.577
outlet D0	98.2	0	0	137	0	0.727
inlet EP	97.7	1024	16	382	426	2.355
outlet EP	96.0	957	14	365	483	1.634
outlet D1	95.8	555	0	161	110	0.701
outlet D1 (+caustic)	89.1	131	0	145	161	0.740
outlet D2	95.4	123	1	236	32	1.144

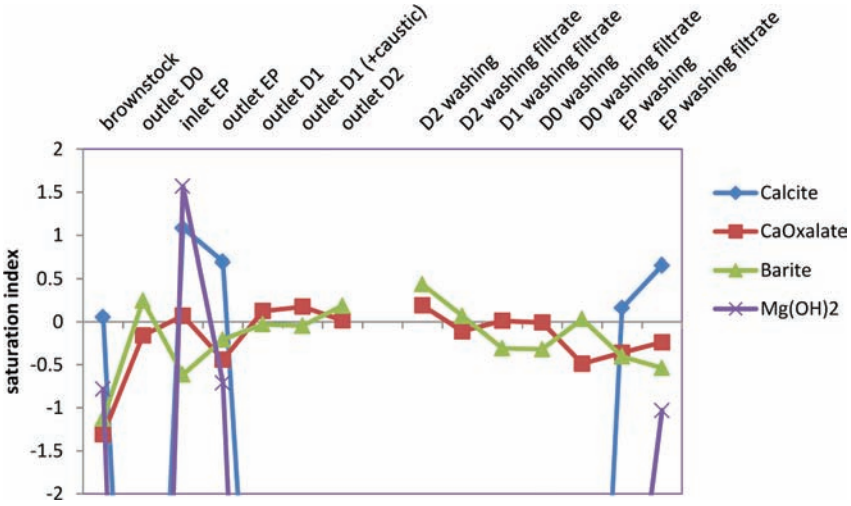

Figure 5. Estimation of local scaling risk (saturation index profiles calculated from water analyses, for the considered mineral phases: Calcite ($CaCO_3$), monohydrated Calcium oxalate ($CaC_2O_4{:}H_2O$), Barite ($BaSO_4$)) and $Mg(OH)_2$. Note that SI(Calcite) and SI($Mg(OH)_2$) are sometimes very low in acidic conditions (SI < –2), therefore not visible on this graph.

The measured distribution of cations between liquid and solid form is given in Figure 7. The partition between precipitated and adsorbed fraction is discussed later on. Calcium enters the bleaching line almost exclusively in solid form with the brownstock. Then all calcium is released to liquid phase in D0 stage. Calcium is again found in solid form in EP stage (as a result of precipitation). Solid calcium

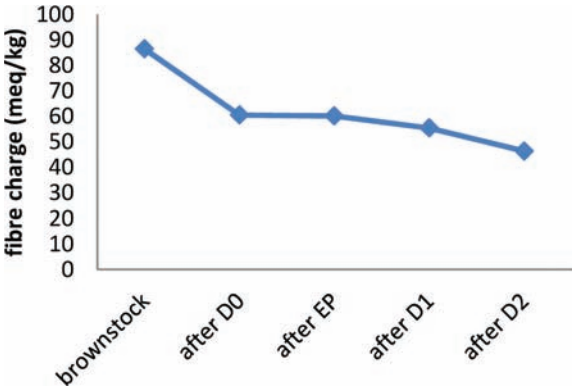

Figure 6. Evolution of fibre charge along the bleaching line.

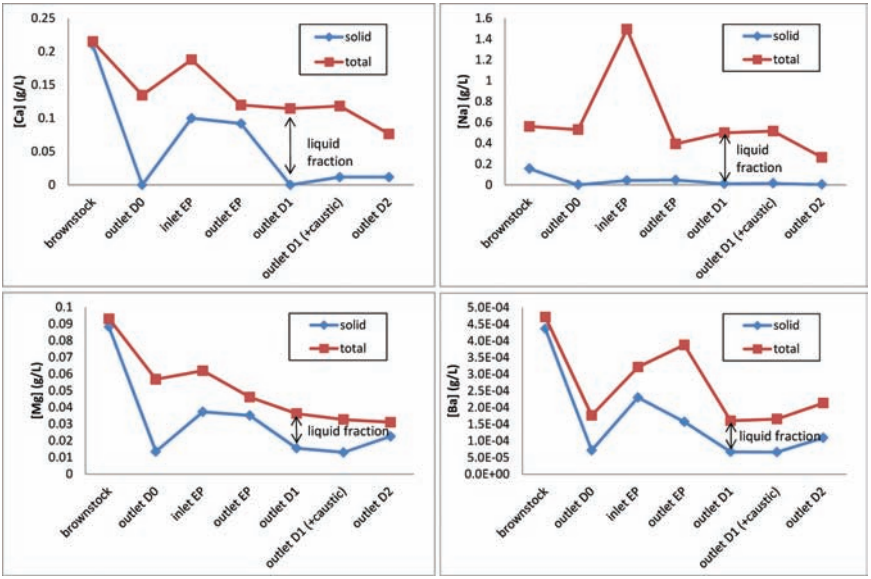

Figure 7. Measured distribution of cations between liquid and solid phase (= adsorbed + precipitated)

is finally dissolved in D1 stage, due to the acidic conditions. Some residual solid calcium is found in D2 stage, possibly in the form of calcium oxalate. The sodium profile shows that, sodium is present mostly in liquid phase, throughout the bleaching sequence. The only solid form of sodium is the fraction adsorbed on

fibres. It can be seen that the adsorbed sodium is not negligible in the conditions of the brownstock. The peak observed at "inlet EP" corresponds to caustic soda injection. The magnesium profile shows that magnesium enters the bleaching line in solid form mostly. It is then dissolved in D0, then reprecipitated in EP, and partially redissolved in D1 stage. The analyses show that barium enters the bleaching line in solid form mostly. That is surprising, as the supersaturation with respect to barite is negative for the conditions of the brownstock, and the amount adsorbed on fibres is not sufficient to explain the measured amount of solid barium. Possibly, the barium is under a solid form other than barite. There is a considerable reduction of total barium after D0 stage: this could be explained by dissolution of the unknown solid barium form, then the released barium precipitates with added sulphate under the form of barite, and some precipitates are separated with the washing filtrates. Further down the bleaching line, the barium concentration remains low, with about an equal partition between liquid and solid form. It is somewhat surprising to find solid barium in inlet EP and D1 stage, as the supersaturation with respect to barite is negative (recall Figure 5).

3.2 Composition of mineral deposits

Deposits are routinely found on the D0 diffuser screen. These were collected and analysed by the mill. They were found to consist mostly of Barite.

The deposit collected from the wall of the pipe to the inlet of the EP diffuser has a layered aspect, with shiny and golden surface. The elemental composition from the X-ray microanalysis is consistent with the formula $CaCO_3$ (by comparison with a pure $CaCO_3$ sample) (Figure 8). The XRD analysis confirms that the deposit has the crystallographic features of Calcite (Figure 9). All these analyses show that the deposit is made of almost pure $CaCO_3$, crystallised in Calcite form.

The deposit collected from EP diffuser screen has a brownish aspect. The elemental composition from the X-ray microanalysis for elemental composition is consistent with the formula CaC_2O_4 (by comparison with a pure CaC_2O_4 sample) (Figure 10). The XRD analysis shows that the deposit has the crystallographic features of Weddellite, a form of dihydrated Calcium oxalate (Figure 11). All these analyses show that the deposit is made of Calcium oxalate, possibly mixed with organic matter, crystallised in Weddellite form.

3.3 Calibration of the simulation model

The resolution of the mass balances simultaneously with all chemical equilibria leads to a good prediction of physico-chemical parameters throughout the bleaching line. That is remarkable as parameters are coupled through the chemical equilibria. For instance, the calculated pH results from chemicals injection,

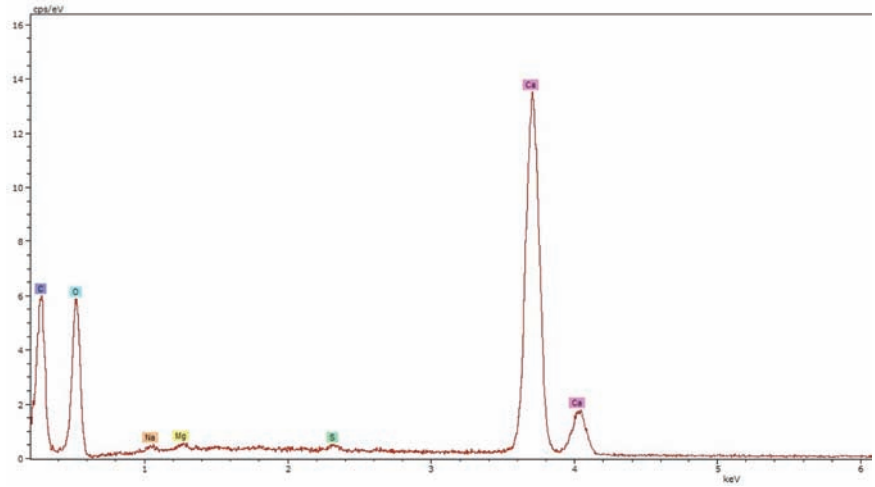

Figure 8. X-ray microanalysis for elemental composition of deposits from pipe to EP after caustic addition.

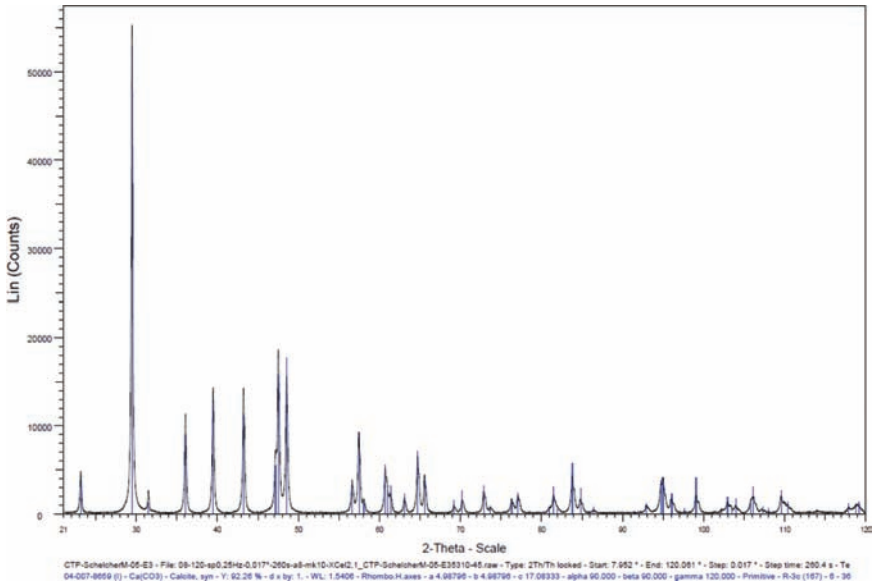

Figure 9. XRD spectrum of deposits from pipe to EP after caustic addition (in blue, characteristic peaks of Calcite).

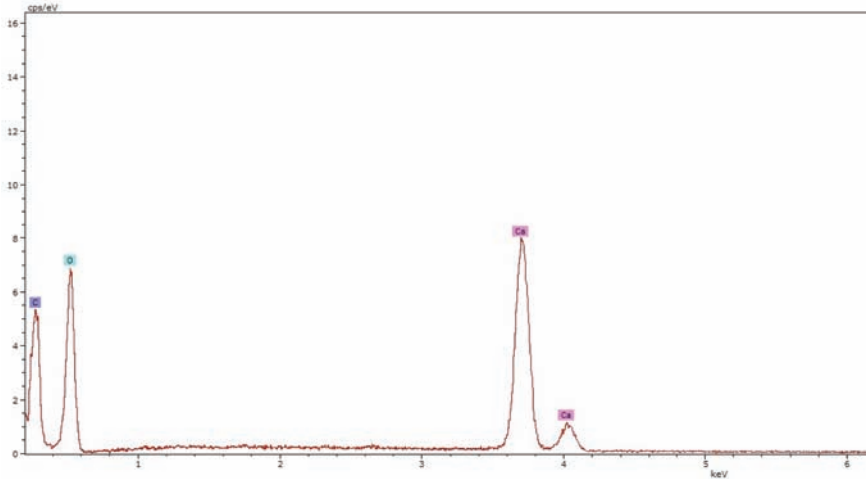

Figure 10. X-ray microanalysis for elemental composition of deposits from EP diffuser.

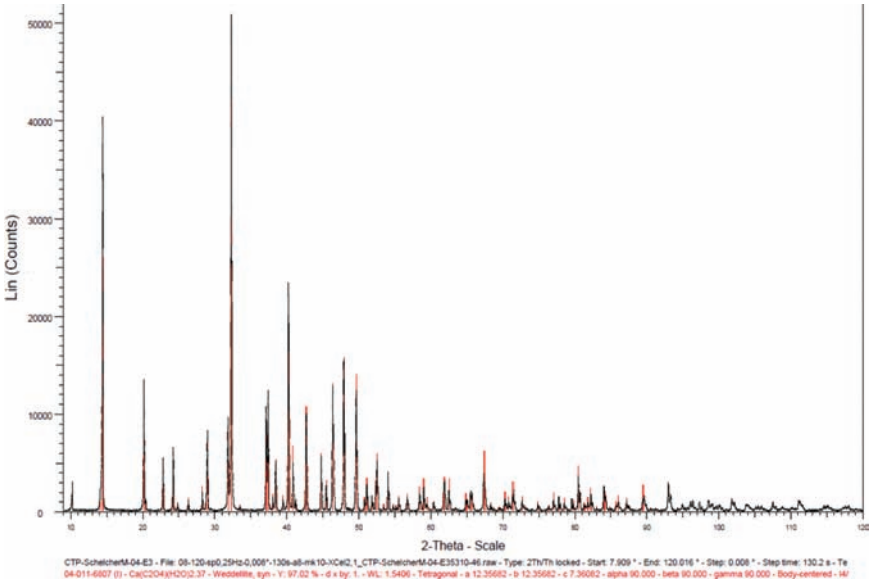

Figure 11. XRD spectra of deposit from EP diffuser (in red, characteristic peaks of Weddellite).

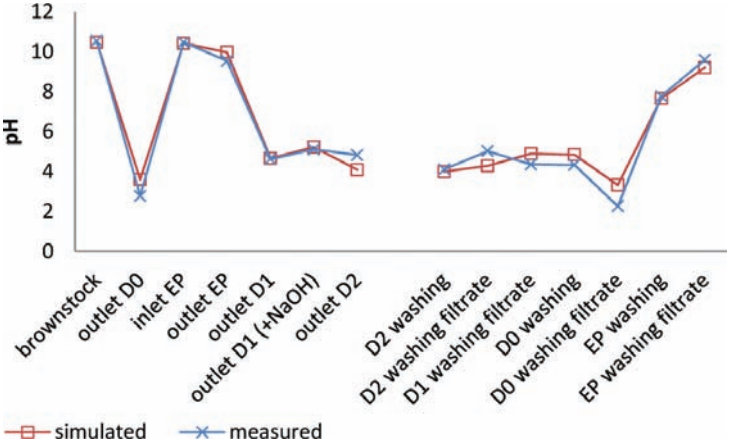

Figure 12. Measured vs. simulated profiles for pH.

release of organic acids, dissolution/precipitation of 3 mineral phases, ion exchange with fibres . . . In other words, it is not possible to fit the various parameters profiles independently from each other.

The implemented numerical methods are quite efficient, so that the full mill model is typically resolved within 10 to 30 s. Therefore, the effect of changing a parameter can be quickly assessed, and multiple scenarios can be tested.

The simulation adequately predicts the pH swings observed in the bleaching line, from alkaline brownstock, to acidic D0 conditions, up to alkaline extraction conditions and down to mildly acidic D1 and D2 conditions (Figure 12). The pH of the effluents is well predicted also.

Simultaneous adjustment of wood organics release and washing efficiency makes it possible to describe accurately the COD profile along the bleaching line (Figure 13). The major COD release that occurs during extraction is well described, together with the displacement washing effect, where the EP filtrate is more concentrated than the washed pulp at EP outlet.

The results of the adjustment of the chemicals injections to the process, together with released wood organics are reported in Table 3. The major COD release occurs during extraction, which is expected. Although the oxidation occurs during D0 stage, the dissolution of organic material takes place during alkaline extraction [34].

The largest oxalate release occurs in D0 stage, then decreases along the next stages. The specific oxalate production in D0 (= 0.77 kg/T) is close to typical values (= 0.6 kg/T) reported in [3]. Oxalate is mostly produced from lignin oxidation, thus roughly proportional to Kappa number reduction over each stage.

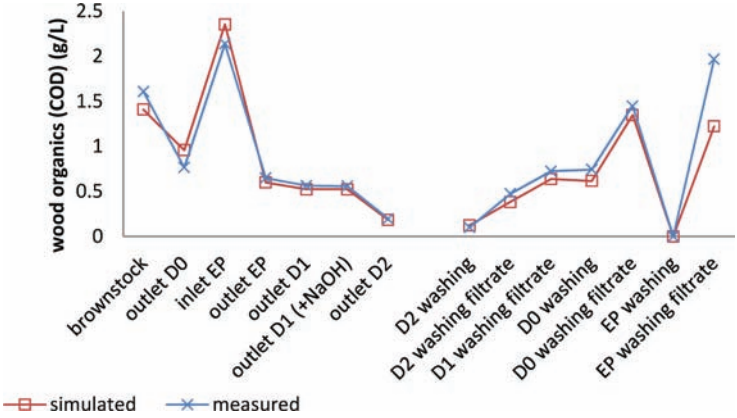

Figure 13. Measured vs. simulated profiles for COD.

A significant source of inorganic carbon is required at EP inlet in order to fit the measured profiles (3.45 kg_CO_2/T). However it is not clear what is the exact source of the inorganic carbon. Possibly, the soda has been carbonated in the preparation process. Upon contact with air, the undersaturated caustic soda naturally sucks CO_2 from the atmosphere. The carbonatation phenomena can be very quick. Another hypothesis is that inorganic carbon is formed from partial mineralisation of organic matter in alkaline oxidative conditions. There is very little literature on this topic. However, in ref. [35] it is shown that inorganic carbon can be formed from lignin oxidation reactions during peroxide bleaching. From their data, 1g of lignin forms 0.044 g of dissolved CO_2. With an estimated lignin content of 0.5% (Kappa = 3.5), this corresponds to 0.22 kg_CO_2/T. This is lower than the identified inorganic carbon source.

The sodium sulphate and sulphuric acid in the spent acid are close to a 50:50 ratio, which is expected from the Mathieson process for chlorine dioxide production: $2NaClO_2 + SO_2 + H_2SO_4 = 2ClO_2 + 2NaHSO_4$, with spent acid: $2NaHSO_4 = Na_2SO_4 + H_2SO_4$.

The washing efficiencies calculated from the diffusion washer model are given in Table 4. The most efficient displacement of liquor occurs in D2 diffuser (DR = 0.84). Although the extraction stage is washed with raw water, and using a high dilution factor (DF = 3.83), it has a poorer displacement ratio (DR = 0.75). The parameter C_t allows to compare displacement efficiencies, independently of DF. The poorest C_t is observed for the D1 washer (= 15%), and the highest C_t for the D2 washer (= 30%).

In order to understand the formation of mineral deposits, the calcium profile is firstly studied together with the inorganic carbon profile (Figure 14 and Figure 15).

Table 3. Specific release of wood organics and chemicals injection to the simulated process (kg/T)

	kg/T COD	kg/T *Oxalate*	kg/T CO_2	kg/T Na_2SO_4	kg/T H_2SO_4	kg/T NaOH
D0	7.30	0.77	0.00	13.13	15.07	0.00
EP	13.07	0.33	3.45	0.00	0.00	18.16
D1	2.90	0.11	0.00	1.42	1.63	0.00
D2	0.00	0.07	0.00	0.00	0.00	0.35

Table 4. Washing parameters of the simulated process (F_w (m^3/h): wash water flow, P (T/h): pulp production = 27.7 o.d.T/h, C_t (%): intermediate thickening concentration, C_{wp} (%): washed pulp concentration, DF: dilution factor, DR: displacement ratio)

	Fw/P (m^3/T)	Ct (%)	Cwp (%)	DF	DR
D0	11.55	18	9.8	2.35	0.72
EP	13.36	18	9.5	3.83	0.75
D1	12.27	15	8.9	2.04	0.68
D2	12.64	30	9.4	3.00	0.84

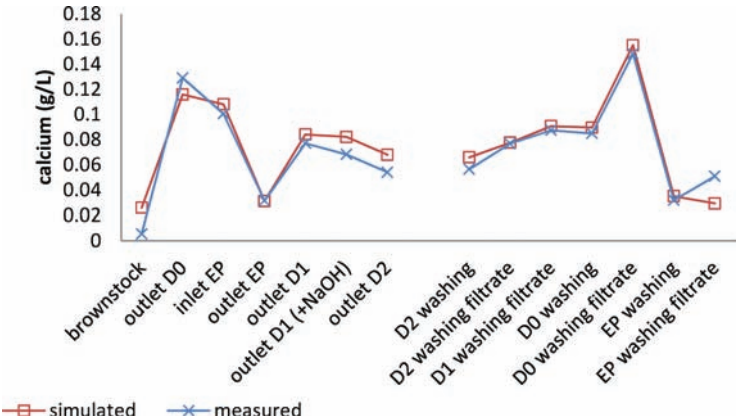

Figure 14. Measured vs. simulated profiles for total dissolved calcium.

Dissolved calcium is low in the brownstock, as most calcium is under solid form in these alkaline conditions (recall Figure 7). On the other hand, the inorganic carbon reaches high level. Upon acidification in D0 stage, most solid calcium is dissolved to liquid phase. Note that the fraction of calcium that was adsorbed on

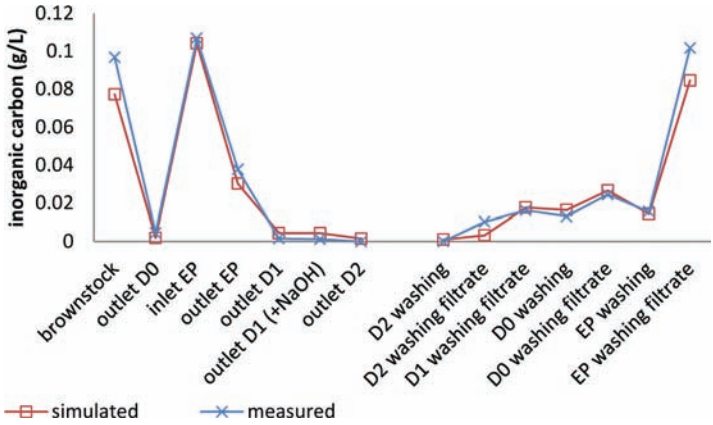

Figure 15. Measured vs. simulated profiles for total inorganic carbon.

fibres is released to the liquid phase as the fibre gets protonated, and this somewhat contributes to rising dissolved calcium level. The inorganic carbon goes down to almost zero at the same time. That can be explained by degassing in the atmospheric diffuser, as the cascade of carbonic equilibria is displaced towards dissolved CO_2 in acidic conditions. Right after caustic soda injection, the inorganic carbon rises dramatically. In the simulation, this was well described by introducing a CO_2 source. This is representative of soda carbonatation, and possibly mineralisation of organic matter, as discussed above. This causes a high supersaturation with respect to calcium carbonate. If we allow that local precipitation of calcite in the simulation, we are able to reproduce both calcium and inorganic carbon profiles anywhere in the circuits. Note that the precipitation does not proceed to full equilibrium, as we had to set SI(calcite) = 0.3 to reproduce the observed profiles. There is possibly a kinetic limitation by the residence time in the EP diffuser. If we do not allow the precipitation to occur, the washing effect is not sufficient to explain the calcium decrease after EP, the calcium level gets too low in D1 and D2 stages, and the pH gets too acidic. Thus, the model shows that precipitation of calcite is the most likely explanation for the observed decrease of dissolved calcium after extraction. Inorganic carbon also decreases after extraction for the same reason. The Calcite precipitates (about 2 kg/T) must be set to follow the pulp flow to explain observed profiles down the bleaching line. Indeed, they play the role of a calcium source upon acidification in D1 stage. That explains the observed increase in D1 stage, that is further maintained in D2 stage. Note that in the washing process, calcium is distributed between the pulp and the filtrates based only on chemical reactions. This determines the amount that goes back to previous stages through counter-

current washing. These loop effects contribute to the build-up of calcium in the D0-D1 loop, and are well described by the model.

The oxalate profile (Figure 16) is also linked to the calcium profile. The oxalate concentration rises at D0 outlet, although the pulp has been washed. That is due to the considerable release of oxalic acid that occurs in D0 conditions. The oxalate level further increases in EP inlet. Together with the high corresponding dissolved calcium level, the chemical speciation indicates that the flow gets supersaturated with respect to calcium oxalate. Thus precipitates of calcium oxalate are formed down to SI(Calcium oxalate) = 0. However, the model indicates that the supersaturation level is quite limited, and that the amount of formed oxalate deposits is low (= 0.15 kg/T). This suggests that the problems related to calcium oxalate deposits in EP stage could be solved with limited actions on the process. The simulation also predicts a slight formation of calcium oxalate in D2 stage, which does not seem to cause deposits in the mill case.

All in all, the simulation provides a good description of solid calcium profiles as well (Figure 22). Evaluation of precipitated amounts shows that it is mostly explained by the calcite precipitation phenomena.

Risks of barite deposits can be evaluated by studying both the barium and sulphate profiles (Figure 17 and Figure 18). It was possible to explain the general evolution for dissolved barium. The description of solid barium profile is however not fully satisfactory (Figure 22).

The measured solid barium content remains higher than the simulated precipitated barite in the brownstock, as already discussed. Further down the bleaching line, the simulation predicts that barite dissolves in EP conditions then reprecipitates in further D1 and D2 conditions. On the other hand, the measurements show

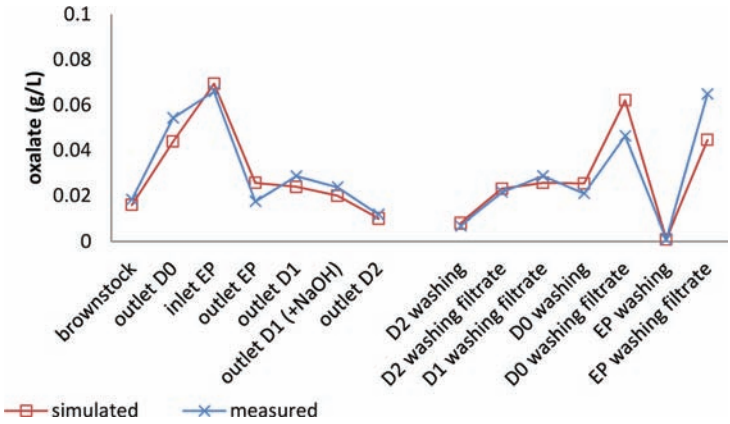

Figure 16. Measured vs. simulated profiles for total dissolved oxalate.

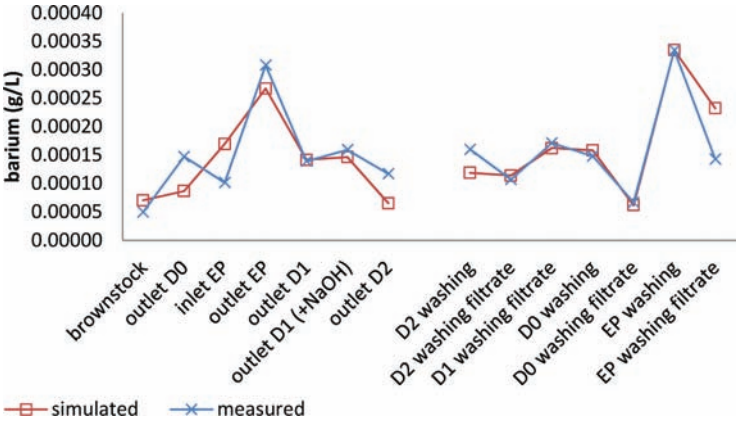

Figure 17. Measured vs. simulated profiles for total dissolved barium.

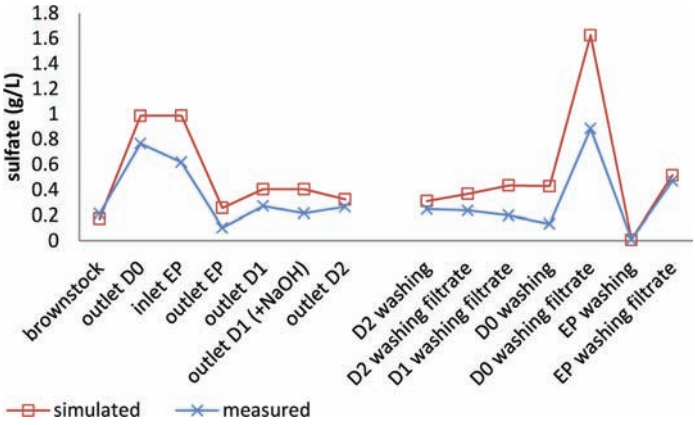

Figure 18. Measured vs. simulated profiles for total dissolved sulphate.

that Barite behaves like an inert mineral once it has been formed. In other words, it does not redissolve when the flow gets under-saturated. Same effect has been mentioned in [31] which mentions that "it is not likely that the barium sulphate that precipitates in the cook would redissolve to any large extent under the acidic conditions in the D-stage, and again precipitate to cause deposits." The general evolution of the sulphate profile is captured by the simulation.

The incoming total measured barium in the brownstock is about 4 ppm (on dry pulp). This value is rather typical for such process. In [4], reported values range from 9 to 25 ppm for a D0 stage. Recall that wood chips are the only source

of barium to the process, with hardwood chips containing usually 20–60 ppm and softwood about 10 ppm.

The simulation could reproduce both the measured dissolved magnesium level (Figure 19) and solid magnesium profile (Figure 22). Magnesium is present mostly under solid form in the brownstock as magnesium hydroxide. It is then dissolved in D0 acidic conditions. Magnesium again precipitates in alkaline extraction conditions. The formed precipitates are transferred to the D1 stage and redissolved. The only discrepancy between the measurement and the simulation concerns the "inlet EP" sample, where predicted dissolved magnesium is too low. It is believed that this is due to kinetic limitation on the formation of magnesium hydroxide: the precipitate may fully form later on in the bleaching tower, whereas the simulation calculates instant precipitation equilibrium at the inlet of the tower. Note that both dissolved and solid magnesium are adequately predicted at the outlet of the extraction tower.

Magnesium is not directly involved in typical mineral deposits issues, but may affect the formation of other deposits through complexation effects (especially with oxalate), or by competition with other metal cations for adsorption on fibres.

The dissolved sodium profile (Figure 20) could be well predicted by the simulation. The high peak at "inlet EP" of course corresponds to caustic soda injection. The solid sodium profile (Figure 22) is also well described, except at "outlet EP", where the value is under estimated. Sodium does not participate in any mineral deposits, so that solid sodium corresponds to adsorbed sodium. Thus it can displace cations from the fibres (such as calcium and barium), which are then available for precipitation. It also complexes with inorganic carbon in hot alkaline conditions, which modifies carbonate activity in EP stage. This directly reduces the supersaturation with respect to Calcite, hence the associated deposits.

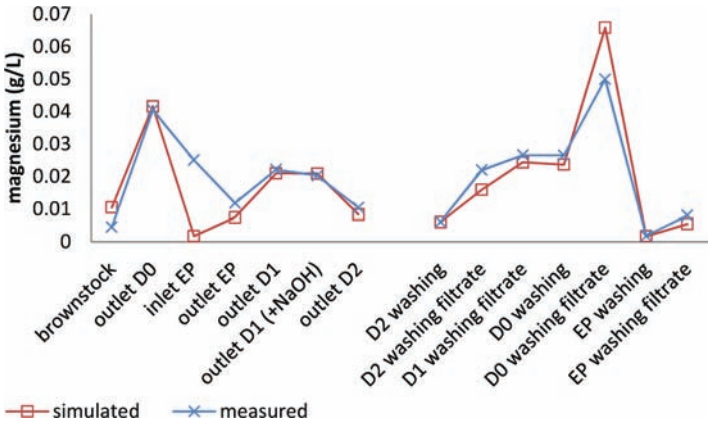

Figure 19. Measured vs. simulated profiles for total dissolved magnesium.

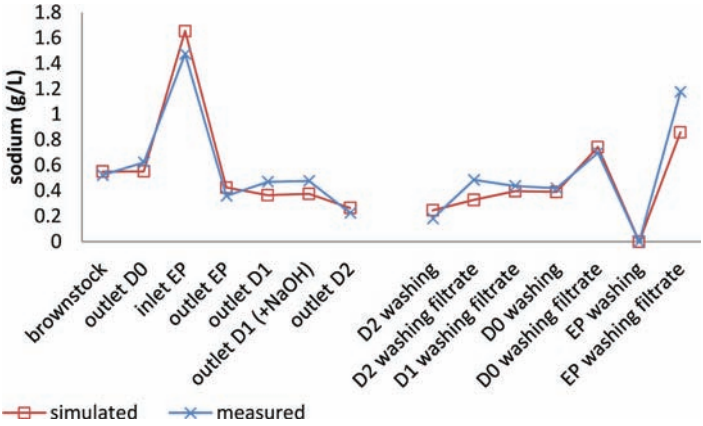

Figure 20. Measured vs. simulated profiles for total dissolved sodium.

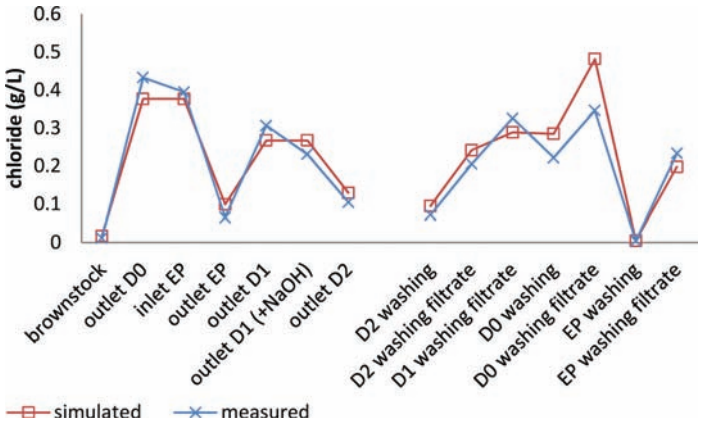

Figure 21. Measured vs. simulated profiles for total dissolved chloride.

The general evolution of chloride could be described as well (Figure 21). Remember that in our simulation, chloride is only a tracer representative of chlorine species.

The calculated amounts of adsorbed cations are reported in Figure 23. In general, sodium is the major adsorbed cation on fibres. The affinity of sodium for fibres is not particularly high, but the sodium concentration is quite high so that it adsorbs in large amounts. Barium represents a small amount of total adsorbed cations. As expected the highest total amount of adsorbed cations is found in the brownstock. The desorption of cations in D0 stage due to acidic conditions is

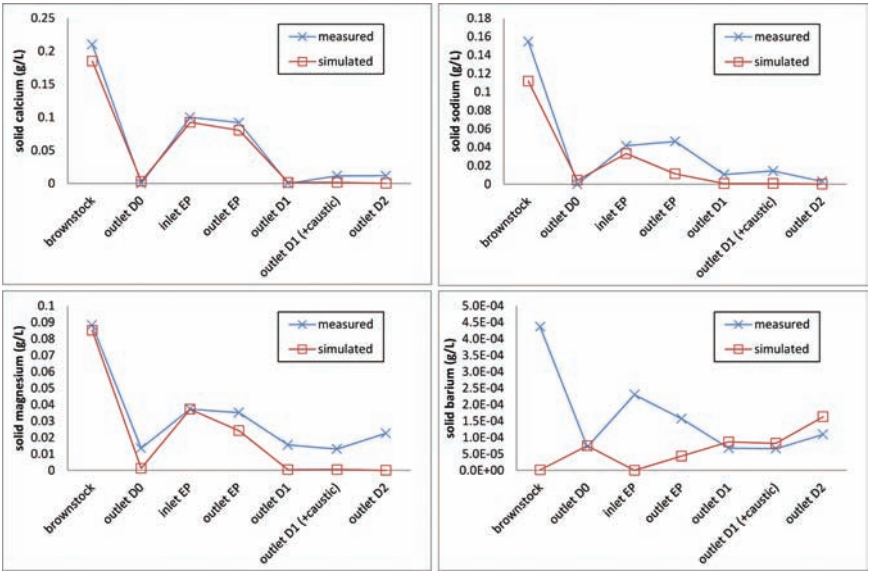

Figure 22. Measured vs. simulated total solid cations (= adsorbed + precipitated).

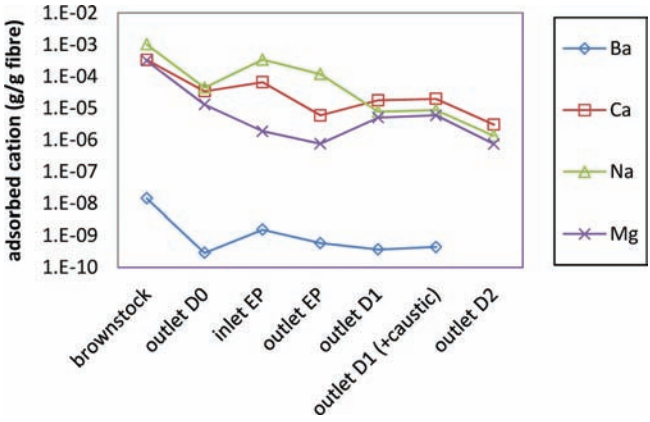

Figure 23. Distribution of cations adsorbed on fibres (calculated).

clearly visible for all cations. This releases a significant amount of cations to the liquid phase, which are available for precipitation. Increasing the pH in alkaline extraction favours the re-adsorption of cations. Further down the line, the adsorbed amounts are modified by precipitation phenomena.

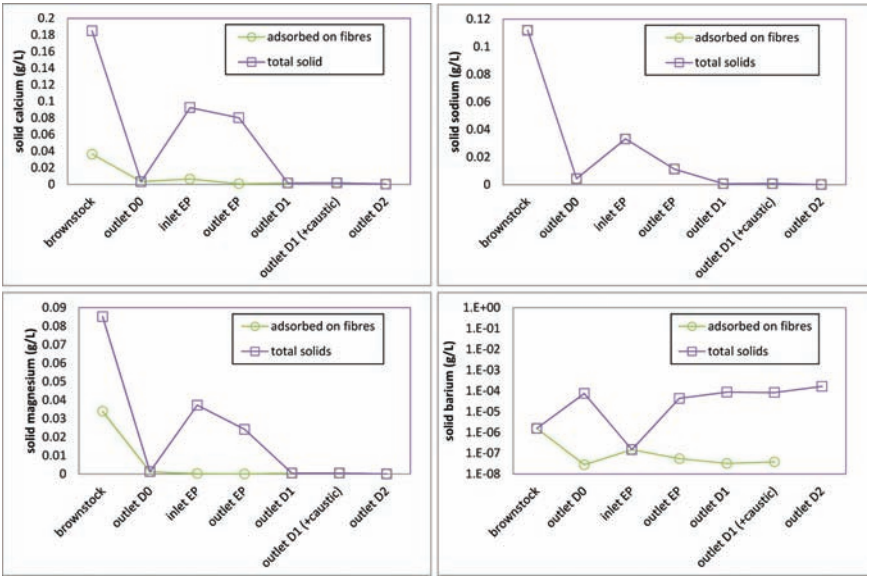

Figure 24. Fraction of solid cations adsorbed on fibres (calculated).

The contribution of adsorbed cations to total solids is plotted in Figure 24. The adsorbed calcium in the brownstock represents about 25% of solid calcium and also about 25% of total calcium (as it is mostly in solid form). Then it decreases to a much lower fraction. As already mentioned, adsorbed sodium is equal to 100% of solid sodium in the simulation, which represents 25% of total sodium in the brownstock. Adsorbed barium represents only a small fraction of total barium, as it has low affinity with fibres.

3.4 Simulation of curative solutions to mineral deposits

3.4.1 Barium sulphate deposits

The easiest way to limit barite deposits, is to limit the source of sulphate to the process. As the mill uses spent acid ($NaHSO_4$) to acidify the pulp at D0 inlet, it could be tempting to try to use other types of acids containing less sulphate. Firstly, we have simulated the substitution of NaHSO4 by pure H_2SO_4: this reduces sulphate content by a factor 2 per added proton. This strategy reduces barite deposits, but is not sufficient to suppress deposits (Table 5). Furthermore, we have simulated the replacement of the spent acid with HCl, which does not contain any sulphate. This would indeed totally suppress barite deposits.

Table 5. Effect of acid type used for pH regulation on Barite deposits at D0 (simulated)

Acid	kg/T Na_2SO_4	kg/T H_2SO_4	kg/T HCl	pH	g/T $BaSO_4$ *deposits*
Spent liquor	13.05	14.97	0.00	3.12	0.25
H_2SO_4	0.00	14.89	0.00	3.12	0.09
HCl	0.00	0.00	10.84	3.12	0.00

3.4.2 Calcium carbonate deposits

One possibility to limit the formation of calcite deposits in EP stage is to decrease the source of inorganic carbon associated to the caustic soda addition. The simulation allows to calculate the global effects of reducing the injected CO_2 flow rate (Figure 25). It demonstrates that it is indeed an efficient way to reduce formed Calcite. Therefore limiting soda carbonatation during the preparation process would greatly help limiting calcite deposits in the pipe to EP inlet.

3.4.3 Calcium oxalate deposits

From the scaling point of view, introducing magnesium into the system has great potential advantages. The introduction of magnesium salts is a large source of Mg^{+2} that competes with Ca^{+2} in the formation of calcium oxalate deposits. Magnesium forms soluble magnesium oxalate complex (log(K) = 3.56). Therefore less oxalate is available to precipitate with calcium. This offers opportunities for reducing calcium oxalate deposits by using alternative alkali sources such as $Mg(OH)_2$, MgO or magnesium salts such as $MgCl_2$ or $MgSO_4$.

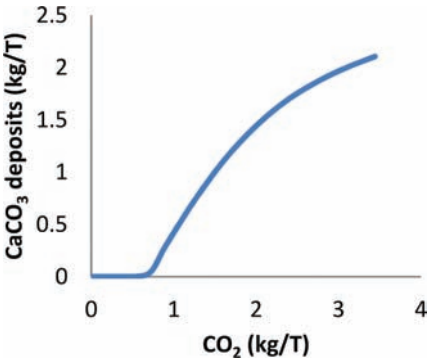

Figure 25. Influence of inorganic carbon source reduction at EP inlet on calcite deposits (simulated).

We have simulated the partial substitution of NaOH by MgO at EP inlet (Figure 26). Based on equivalent alkali, 2 kg/T of NaOH were replaced by 1 kg/T of MgO. Results show that only a minor addition of MgO (1 kg/T) may inhibit totally the formation of Calcium Oxalate at extraction stage. That is due to the fact that the pulp flow is only slightly supersaturated with respect to calcium oxalate. This scenario (noted "A" in the following, see Table 6) also lowers the end pH of the extraction stage (from 10.4 to 9.7). This has been observed experimentally with caustic soda substitution by magnesium oxide [22], [23], and can be attributed to the limited solubility of the formed magnesium hydroxide. According to our experience, brightness could be maintained, even with this reduced pH [25].

Substitution scenario A suppresses calcium oxalate deposits in EP stage. It also greatly lowers calcium oxalate deposits at D1 and D2 stage (as predicted by the reference simulation, see Figure 27), but does not suppress them. In addition, the simulation predicts that partial substitution of caustic soda by magnesium oxide at extraction stage has consequences further down the bleaching line: the pH at D1 inlet increases largely (from 5.2 to 8.2), which is not acceptable. That is because solid magnesium hydroxide formed at extraction is transferred to the next acidic loop and buffers the pH upon redissolution. Adjusting the sulfuric acid used for pH regulation at D1 inlet is not recommended as this would further lower the pH of the extraction stage through loop effects (not shown). The problem could be solved by shutting down the caustic soda used for pH regulation at D2 inlet (scenario B in Table 6). Interestingly, this action also allowed to totally suppress calcium oxalate deposits in D1 and D2 stages.

Note that the proposed scenarios to suppress calcium oxalate have very limited impact on deposition tendency of calcite and barite (not shown).

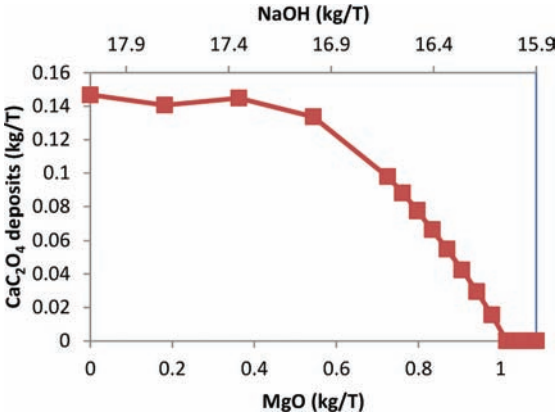

Figure 26. Influence of partial substitution of NaOH by MgO at EP stage on local calcium oxalate deposits (simulated).

Table 6. Simulated scenarios for reducing of calcium oxalate deposits

	EP inlet MgO (kg/T)	*EP inlet* NaOH (kg/T)	EP inlet pH	D2 inlet NaOH (kg/T)	D2 inlet pH
ref	0.00	18.14	10.42	0.18	5.23
scenario A	1.02	16.11	9.66	0.18	8.18
scenario B	1.02	16.11	9.65	0.00	5.08

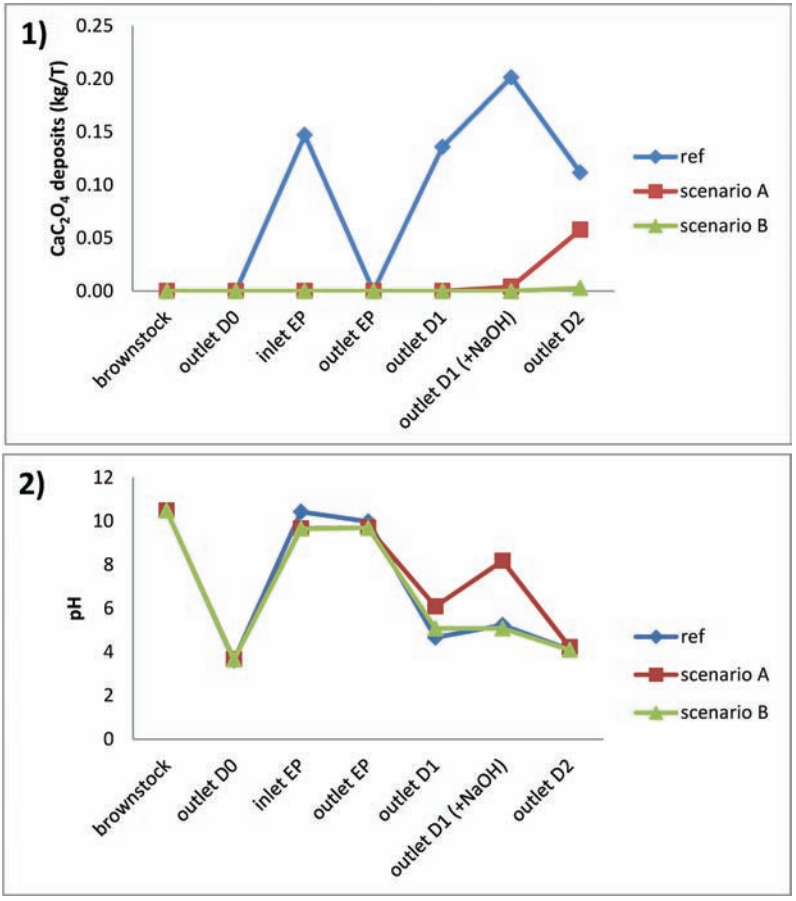

Figure 27. Effects of simulation scenarios on (1) calcium oxalate deposits throughout the bleaching line and (2) pH profiles.

4 CONCLUSIONS

A chemical process simulation of mineral deposits in kraft pulp bleaching line has been developed.

The simulation handles a 3 phase system (solid-liquid-gas phases). The 4 considered mineral phases (Calcium carbonate, calcium oxalate, barium sulphate and magnesium hydroxide) can dissolve in, or precipitate from the liquid phase. Ion exchange capacity of fibres is considered with respect to calcium, sodium, barium and magnesium. Complexation effects of calcium and barium with wood organics released during bleaching reactions are taken into account. The injection of chemicals such as caustic soda or sulfuric acid can be simulated. The gaseous exchanges with atmospheric CO_2 are simulated as well. The pH resulting from all these chemical equilibria is calculated and propagated in the circuits.

The model has been calibrated against field measurements. The model describes the D0(EP)D1D2 bleaching sequence of the Fibre Excellence Saint Gaudens mill. The resolution of the mass balances simultaneously with all chemical equilibria leads to a good prediction of physico-chemical parameters throughout the bleaching line. For instance, the simulation adequately predicts the pH swings observed in the bleaching line, from acidic conditions in D0 stage, to alkaline conditions of EP stage. That is achieved with a limited number of adjustable parameters, such as washing efficiency in the diffuser model. Most selective separation effects in model blocks are governed by chemical equilibria.

The simulation predicts risks of barite deposits in D0, D1 and D2 stages. The mill did report barite related problems on D0 diffuser screen. The simulation also predicts deposits of calcite at the inlet of the EP stage. This is corroborated by mill observations and analyses of deposit samples. The simulation also predicts risks of calcium oxalate in the EP, D1 and D2 stages. Deposits of calcium oxalate have been found indeed on the screen of the EP diffuser. However no deposits were found in D1 or D2 stage.

The simulation allows testing curative solutions to reduce mineral deposits. Firstly, the simulation shows that changing the acid used for pH regulation at D0 inlet can limit the formation of barite deposits. Secondly, reducing caustic soda carbonatation would largely limit the formation of calcite deposits in EP inlet. Finally, the simulation predicts that it is possible to suppress calcium oxalate deposits throughout the bleaching line by partial substitution of caustic soda by magnesium oxide (1 kg/T) at extraction stage, together with reducing caustic soda used for pH regulation at D2 inlet. The pH profile could be maintained throughout the line (with a pH drop of 0.7 pt at extraction stage that is not anticipated to disturb the bleaching efficiency).

The developed methods are very general and could be applicable to any mill situation, with a limited number of adjustable parameters.

The next step is to include bleaching kinetics, coupled to chemical equilibria. In the present model, the consequences of bleaching reactions are simulated by manually adjusting the release of wood organics. Resolving bleaching kinetic rates will make it possible to predict wood organics generation from lignin degradation rate. Also, the kinetic model will predict Kappa number and ISO brightness as a function of retention time in the bleaching towers.

This will open the way to the development of global simulations of bleaching sequences, able to predict the performance of the process, its consumption and rejects.

ACKNOWLEDGMENTS

Tiphaine Zbogar and Serge Cleyet (CTP) are thanked for experimental work.

Géraldine Champon (Fibre Excellence Saint Gaudens) is thanked for making the field campaign possible.

The authors would like to thank S. Coindeau and T. Encinas from CMTC (Grenoble-INP, France) for XRD measurements and data processing and V. Meyer (CTP) for EDS measurements.

REFERENCES

[1] P. Ulmgren (1997), "Non-process elements in a bleached kraft pulp mill with a high degree of system closure-state of the art," *Nordic Pulp and Paper Research Journal*, **12**(1): 32–41.

[2] M. Häärä, A. Sundberg, and S. Willför (2011), "Calcium oxalate-a source of 'hickey' problems-A literature review on oxalate formation, analysis and scale control," *Nordic Pulp and Paper Research Journal*, **26**(3): 263–282.

[3] A. Elsander, M. Ek, and G. Gellerstedt (2000), "Oxalic acid formation during ECF and TCF bleaching of kraft pulp," *Tappi Journal*, **83**(2): 73–77.

[4] P. S. Bryant, A. Samuelsson, and J. Basta (2003), "Minimizing BaSO4 scale formation in ECF bleach plants," *Tappi Journal*, **2**(3): 3–7.

[5] R. J. Ferguson (2002), "Predicting calcium oxalate scale," in *CORROSION 2002*, Denver, CO.

[6] P. Huber, A. Burnet, and M. Petit-Conil (2014), "Scale deposits in kraft pulp bleach plants with reduced water consumption: A review," *Journal of Environmental Management*, **141**: 36–50.

[7] P. Koukkari, K. Penttilä, K. Hack, and S. Petersen (2000), "CHEMSHEET–An efficient worksheet tool for thermodynamic process simulation," in Y. Bréchet (ed.), *Microstructures, Mechanical Properties and Processes – Computer Simulation and Modelling*, *EUROMAT – Vol. 3*, pp. 323–330.

[8] A. Anderko, P. Wang, and M. Rafal (2002), "Electrolyte solutions: from thermodynamic and transport property models to the simulation of industrial processes," *Fluid Phase Equilibria*, pp. 123–142, 194–197.

[9] P. Wang, A. Anderko, R. D. Springer, J. J. Kosinski and M. M. Lencka (2010), "Modeling chemical and phase equilibria in geochemical systems using a speciation-based model," *Journal of Geochemical Exploration*, **106**(1–3): 219–225.

[10] J. C. L. Meeussen (2003), "ORCHESTRA: An object-oriented framework for implementing chemical equilibrium models," *Environmental Science & Technology*, **37**(6): 1175–1182.

[11] D. L. Parkhurst and C. A. J. Appelo (1999), "User's guide to PHREEQC (version 2)- A computer program for speciation, batch-reaction, one-dimensional transport, and inverse geochemical calculations," USGS Water-Resources Investigations Report, 99–4259.

[12] G. Eriksson (1979), "An algorithm for the computation of aqueous multi-component, multiphase equilibria" *Analytica Chimica Acta*, **112**(4): 375–383.

[13] J. Gustaffson (2006), "Visual Minteq, ver. 2.50," Stockholm: Department of Land and Water Resources Engineering.

[14] A. Kalliola, E. Kukkämäki, R. Pajarre, P. Koukkari, and J. Hakala (2009), "Improving the pH and calcium chemistry control with multiphase modelling, in *Papermaking Research Symposium*, Kuopio, Finland.

[15] P. Kangas, R. Pajarre, M. Nappa, and P. Koukkari (2012), "Multi-phase thermodynamic modelling of pulp suspensions: Review of the methodology," *Nordic Pulp and Paper Research Journal*, **27**(3): 604–612.

[16] Y. Gu, B. Malmberg, and L. Edwards (2004), "Prediction of metals distribution in mill processes, Part 1: Metals equilibrium model," *Tappi Journal*, **3**(1): 26–32.

[17] R. Wadsborn, A. Samuelsson, R. Rådeström, A. Edebo, H. Lendrup, and T. Hedlund-Björnwall (2005), "Metal profiles in the bleach plant: modelling and mill validation," in *2005 Int. Pulp Bleaching Conference*, Stockholm, Sweden.

[18] P. Huber, S. Nivelon, P. Ottenio, and P. Nortier (2013), "Coupling a chemical reaction engine with a mass flow balance process simulation for scaling management in papermaking process waters," *Industrial & Engineering Chemistry Research*, **52**(1): 421–429.

[19] Z. He and Y. Ni (2008), "Peroxide bleaching of eucalyptus CTMP using magnesium hydroxide as the alkali source," *Appita Journal*, **61**(6): 450–455, 460.

[20] L. Yu, M. Rae, and Y. Ni (2004), "Formation of OXALATE from the Mg (OH) 2-Based peroxide bleaching of mechanical pulps," *Journal of Wood Chemistry and Technology*, **24**(4): 341–355.

[21] L. Yu and Y. Ni (2006), "Decreasing calcium oxalate scaling by partial substitution of Mg(OH)2 for NaOH in the peroxide bleaching of mechanical pulps, *Tappi Journal*, **5**(2): 9–12.

[22] A. Gibson and M. Wajer (2003), "The use of magnesium hydroxide as an alkali and cellulose protector in chemical pulp bleaching," *Pulp & Paper Canada*, **104**(11): 28–32.

[23] T. Petrie, A. Gibson, P. Schmidtchen, and M. Wajer (2005), "Magnesium hydroxide: An alternative chemical for pulp bleaching," in *2005 TAPPI Engineering, Pulping, Environmental Conference*, Philadelphia, PA.

[24] L. C. Souza, Y. M. Robles, W. P. Reggiane, and E. C. do Bem (2007), "Sodium hydroxide substitution at bleaching alkaline stage of eucalyptus bleached kraft pulp," in *3rd ICEP International Colloquium on Eucalyptus Pulp*, Belo Horizonte, Brazil.

[25] A. Burnet, L. Savoye, V. Meyer, B. Fabry, B. Carré, and M. Petit-Conil (2014), "Substitution of sodium hydroxide during alkaline bleaching stage of chemical pulp, TMP and DIP," in *Proceedings of the 2014 International Pulp Bleaching Conference*, Grenoble, France, pp. 301–307.

[26] T. Jönsson, R. Radeström, P. Tomani, and P. Ulmgren (1999), "A method for decreasing the risk of calcium oxalate scaling in bleach plants: mill trials and flow sheet simulations," in *Proceedings of the 6th International Conference on New Available Technologies*, Stockholm, Sweden, pp. 194–199.

[27] J. A. Lloyd and C. W. Horne (1993), "The determination of fibre charge and acidic groups of radiata pine pulps," *Nordic Pulp and Paper Research Journal*, **8**(1): 48–52.

[28] A. Mersmann (2001), *Crystallization Technology Handbook. Second Edition Revised and Expanded*. Marcel Dekker.

[29] W. Yantasee (2001), "Kinetic and equilibrium analysis of metal ion adsorption onto bleached and unbleached kraft pulps," PhD Thesis, Oregon State University.

[30] P. Ulmgren and R. Rådeström (2001), "A steady state model describing the solubility of calcium oxalate in D (chlorine dioxide stage)-filtrates," *Nordic Pulp and paper Research Journal*, **16**(4): 389–395.

[31] M. Persson and P. Ulmgren (2002), "Deposition of barium sulfate in bleach plants. Part 1: Solubility and factors affecting the precipitation in D (chlorine dioxide)-filtrates," *Nordic Pulp & Paper Research Journal*, **17**(3): 280–287.

[32] J. Ruiz, P. Ottenio, and B. Carré (2003), "Numerical simulation for Papermakers: CTP capabilities in term of modelling and simulation supported by examples," in *Symposium Simulation & Process Control*, Munich, Germany.

[33] J. Ruiz and P. Ottenio (2006), "Decision support system: Broke ratio management and pulp composition stability," in *Control Systems*, Tampere, Finland, pp. 79–84.

[34] S. Jain, G. Mortha, and C. Calais (2008), "New and Improved Models for All Stages in Full ECF Bleaching Sequences of Softwoods and Hardwoods," in *Tenth International Conference on Computer Modeling and Simulation, 2008. UKSIM 2008*, pp. 272–277.

[35] C. Murphy, G. M. van de Ven Theo, and C. Heitner (2003), "Carbon dioxide evolution during hydrogen peroxide bleaching of lignin-containing pulp," in *ISWPC*, **1**: 101–104.

Transcription of Discussion

PREDICTION OF MINERAL DEPOSITS IN KRAFT PULP BLEACHING LINES THROUGH CHEMICAL PROCESS SIMULATION

Patrick Huber, Sylvie Nivelon, Pascal Ottenio, Matthieu Schelcher and Auphélia Burnet

CTP, CS90251 38044 Grenoble Cedex 9, France

Roger Gaudreault Université de Montréal

It is known that oxalate-based scale is associated with sulphite pulping and/or oxidative bleaching. I would like to know how your software will handle this application?

Patrick Huber CTP, Grenoble

I think one of the big differences with kraft pulp would be the ion exchange capacity of the pulp, which is different for sulphite pulping. The simulation also tracks an ion exchange capacity, so we can adjust for that. Dedicated modules were implemented to control locally the evolution of the ion exchange capacity. For example, the bleaching reaction is affecting the ion exchange capacity, which we can also tune with the simulation.

Roger Gaudreault

Did you validate your model with recycling processes and more specifically wood-free pulping processes? Can you comment on the validity of your model?

Discussion

Patrick Huber

We actually started with recycling processes because we thought it would be easier, there are fewer chemical reactions than in kraft pulp bleaching processes. The pH upsets are not so high, so the first validation was for OCC mills. Here, the main phenomenon is acidification of the process water from anaerobic activity, releasing organic acids to the system, hence partly dissolving calcium carbonate filler. Then we developed it for deinking mills and now for kraft pulp bleaching processes where the situation is much more complex.

Wolfgang Bauer Graz University of Technology

Can you also introduce the chelating agents or complexing agents in your equations?

Patrick Huber

Yes, as long as there is a chemical reaction, we can handle it. The database is open, it's just a text file, so you can insert your new species, new equations, new constants; just re-open the software and it will deal with it. So I have some examples, not shown here, with the use of EDTA for instance in the system.

Wolfgang Bauer

In the line, you were showing there were no complexing agents.

Patrick Huber

No, there weren't any, they don't use it in this mill. In terms of inhibition additives, we can handle anything which works with a chemical reaction. If it works with some dispersing mechanisms or crystal modification that is completely another story. It cannot be handled by these methods and we cannot do it.

Wolfgang Bauer

Did you apply your strategy in the mill and did it work?

Patrick Huber

We have tested it in the lab and yes (I guess you are speaking of magnesium oxide), it gives good results in the lab, but unfortunately we could not test it in

the mill yet. This calibration has been done without magnesium oxide. Not in a mill situation.

Wolfgang Bauer

And the reason why the mill does not want to do it?

Patrick Huber

I don't know precisely. They did not want to modify their process.

Wolfgang Bauer

Maybe they will need the magnesium more.

Thierry Mayade Ahlstrom-Munksjö Apprieu

You said that in some cases, we may have conditions for scaling or precipitation, but we did not find it in the process. Do you think it will be possible that we get the precipitation on the fibre and not on the equipment, and are there ways to predict that?

Patrick Huber

The first part of the answer is, hopefully, yes. If all the precipitates formed on the washer, it just would be impossible to run the mill so it is difficult to estimate, but possibly 95% of the precipitates follows the pulp flow and does not form deposits, hopefully. Only a fraction of it is forming on the pipes and the washer. It is very difficult to estimate how much we deposit and how much we do not deposit, and it requires very different methods than solving a chemical equilibrium. The affinity for the surfaces, nucleation regime, etc., is a very different story.

Jose Iribarne WestRock

How did you model the dissolution time and precipitation time; in other words the reaction times, because that can give you a clue on the previous question?

Patrick Huber

I have not mentioned, but it is written in the paper. By default, all reactions go down to equilibrium, so the barite, the calcium oxalate, do dissolve or precipitate

instantly towards equilibrium in the simulation. As you can see from the result, it seems to be the case. For calcite, we know it is different. Calcite requires a high supersaturation to trigger the nucleation and to start depositing and it does not go down to equilibrium. So for calcium carbonate, it is a bit different, we allow supersaturation. It stays supersaturated and does not precipitate, and at some locations we allow precipitation down to some target saturation index and this is able to reproduce the observed profiles. It is not fully satisfactory, I agree, but this is approximately what happens in a mill, with a very quick equilibrium for everything except for calcium.